Supplemental Figure 1

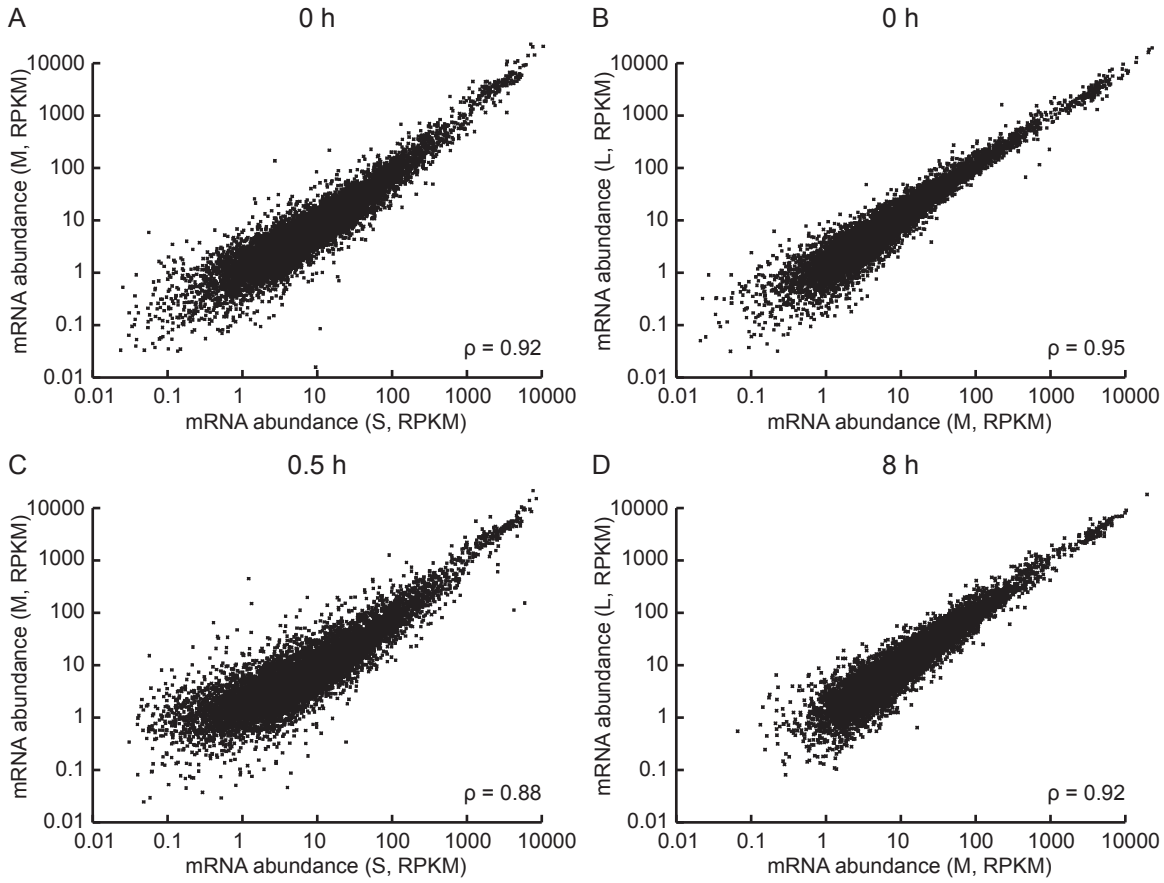

Supplemental Figure 1: Comparison of mRNA expression estimates between different biological replicates of Chlamydomonas strain CC4532

Cells of Chlamydomonas strain CC4532 were collected at the indicated time point after transfer to N-free medium, mRNA was purified and cDNA was generated for RNA-Seq analysis. Expression estimates of the Au10.2 gene models are reported in units of RPKM (Mortazavi et al., 2008). Expression estimates for each of the 12338 expressed genes were compared between two replicates and plotted on logarithmic scales on y and x axis, respectively. The Spearmans rank correlation coefficient (ρ) was calculated and is presented in the figure. Comparison of nitrogen-replete samples (0 h) between 1 h and 8 h time course (A), nitrogen-replete samples (0 h) between 8 h and 48 h time course (B), 30 min nitrogen-deprived samples between 1 h and 8 h time course (C) and 8 h nitrogen-deprived samples between 8 h and 48 h time course (D).

Supplemental Figure 2

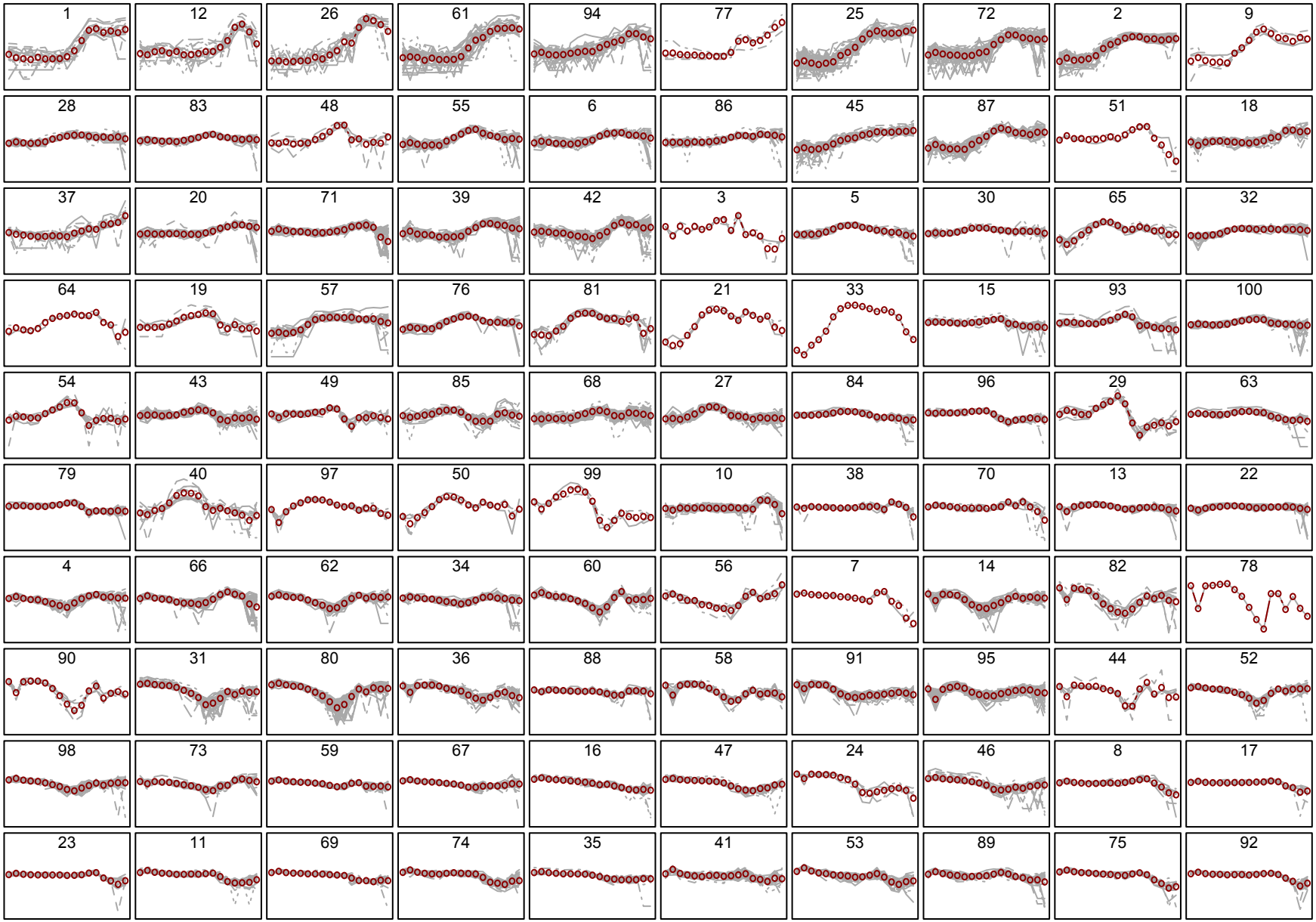

Supplemental Figure 2: Clustering of 4288 differentially expressed genes identified in the CC4532 RNA-Seq experiments

A model-based clustering approach was used to group the 4288 differential expressed genes from the RNA-Seq data in Chlamydomonas strain CC4532 (MBClusterSeq) into 100 clusters. The figure shows the expression patterns for all significantly differentially expressed genes in each cluster for the following 16 time points: +N, 0, 2, 4, 8, 12, 18, 24, 30, 45, 60 min (from the 1 h experiment), 4 h (from the 8 h experiment) and 8, 12, 24, 48 h (from the 48 h experiment). The y-axis represents the $\log_2$ fold changes relative to the mean expression across all time points for each gene. Red circles indicate average fold changes within each particular cluster.

Supplemental Figure 3

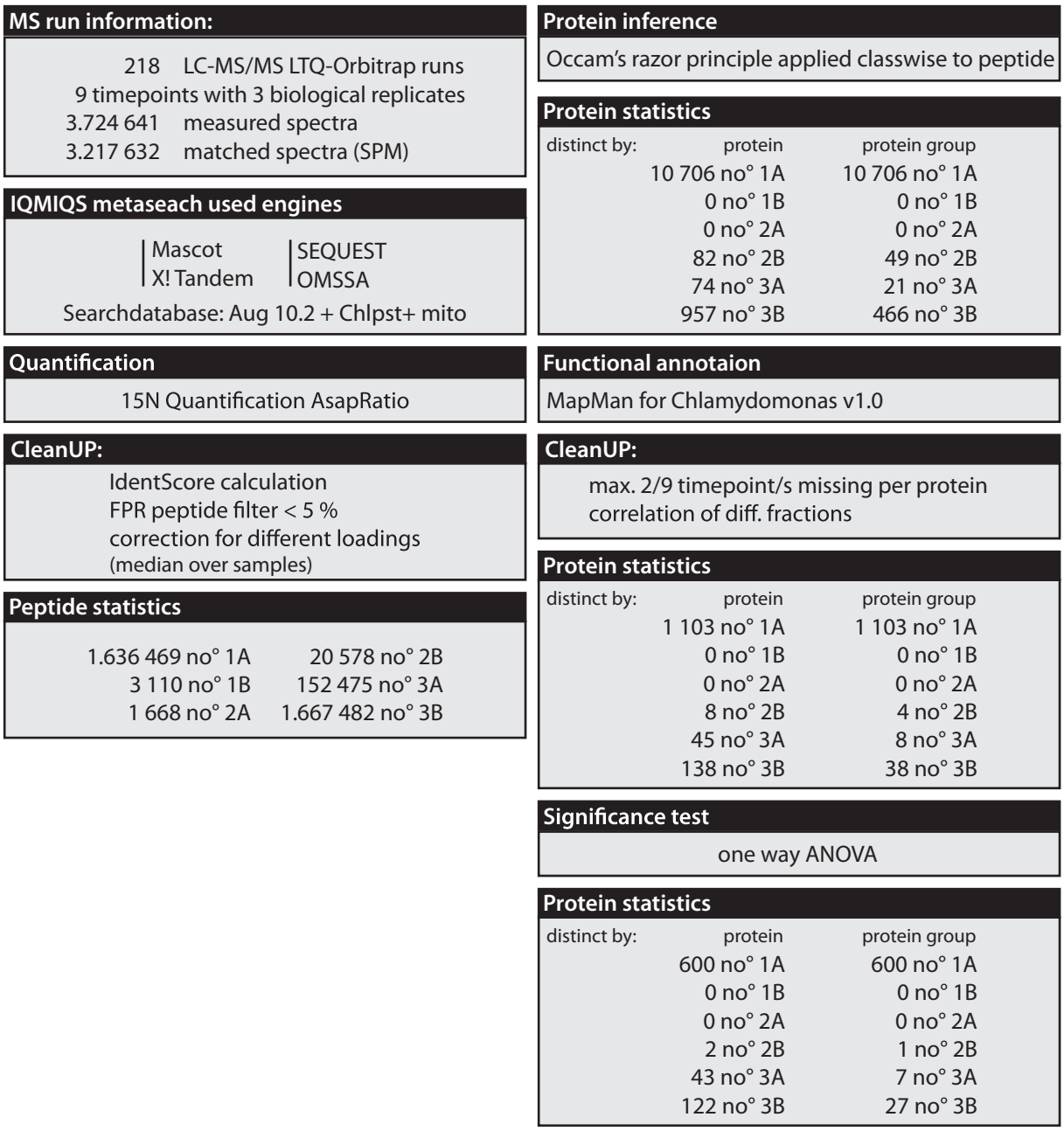

Supplemental Figure 3: Summary of the experimental data gathered from the proteomics time-course experiment

A total of 3,724,641 spectra were detected in 218 120 min-long chromatographic separations and subsequent tandem mass spectrometry runs. Using IOMIQS metasearch, that facilitates four different search algorithms (Mascot (Perkins et al., 1999), Sequest (Eng et al., 1994), OMSSA (Geer et al., 2004) and X!Tandem (Craig and Beavis, 2004)), we were able to match 1,636,469 spectra to class 1a peptide sequences, as well as 3,110 SPMs to class 1b, 1,668 SPMs to class 2a, 20,578 SPMs to class 2b, 152,475 spectra to class 3a peptides and 1,667,482 SPMs to class 3b, according to the classification principles of (Qeli and Ahrens, 2010). After filtering at the peptide level by a false positive threshold < 5 %, the protein identifications were further filtered by removing protein or protein groups with fewer than 7 identification out of 9 time points. The filtration resulted in 1,153 mainly class 1a proteins. For peptide quantification ^{15}N metabolic labeling with a uniform ^{15}N-labeled standard (Mühlhaus et al., 2011) and the algorithm ASAPRatio (Li et al., 2003) were used. Analysis of variance (ANOVA) over time revealed 635 protein groups differentially regulated.

Supplemental Figure 4

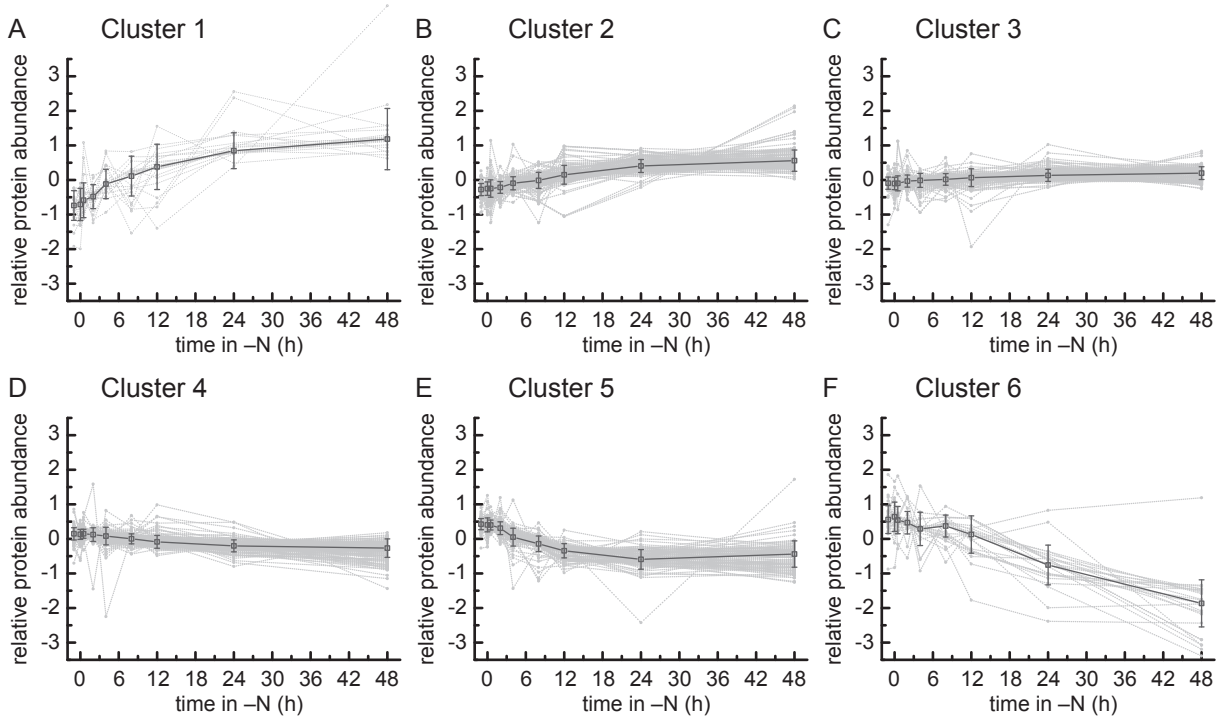

Supplemental Figure 4: Clustering of 635 differentially accumulating proteins upon transfer to N-free media

The centered protein changes were clustered using *k*-means algorithm with euclidean distance metric. The number of cluster was determined using gap statistic taking into account the original dataset's shape (Tibshirani et al., 2001). Gap statistic suggested two major trends within the protein data which can be further split in 6 clusters for a more detailed visualization of the temporal expression. The clusters are sorted from strong increased (A) to strong decreased abundance (F). Plotted is the $^{14}N/^{15}N$ ratio on a $\log_2$ transformed scale at the indicated time point after transfer to nitrogen-free media of each protein within the cluster (light grey) as well as the median ratio (dark grey). Error bars indicate standard deviation between all proteins within the cluster.

Supplemental Figure 5: Photosynthesis

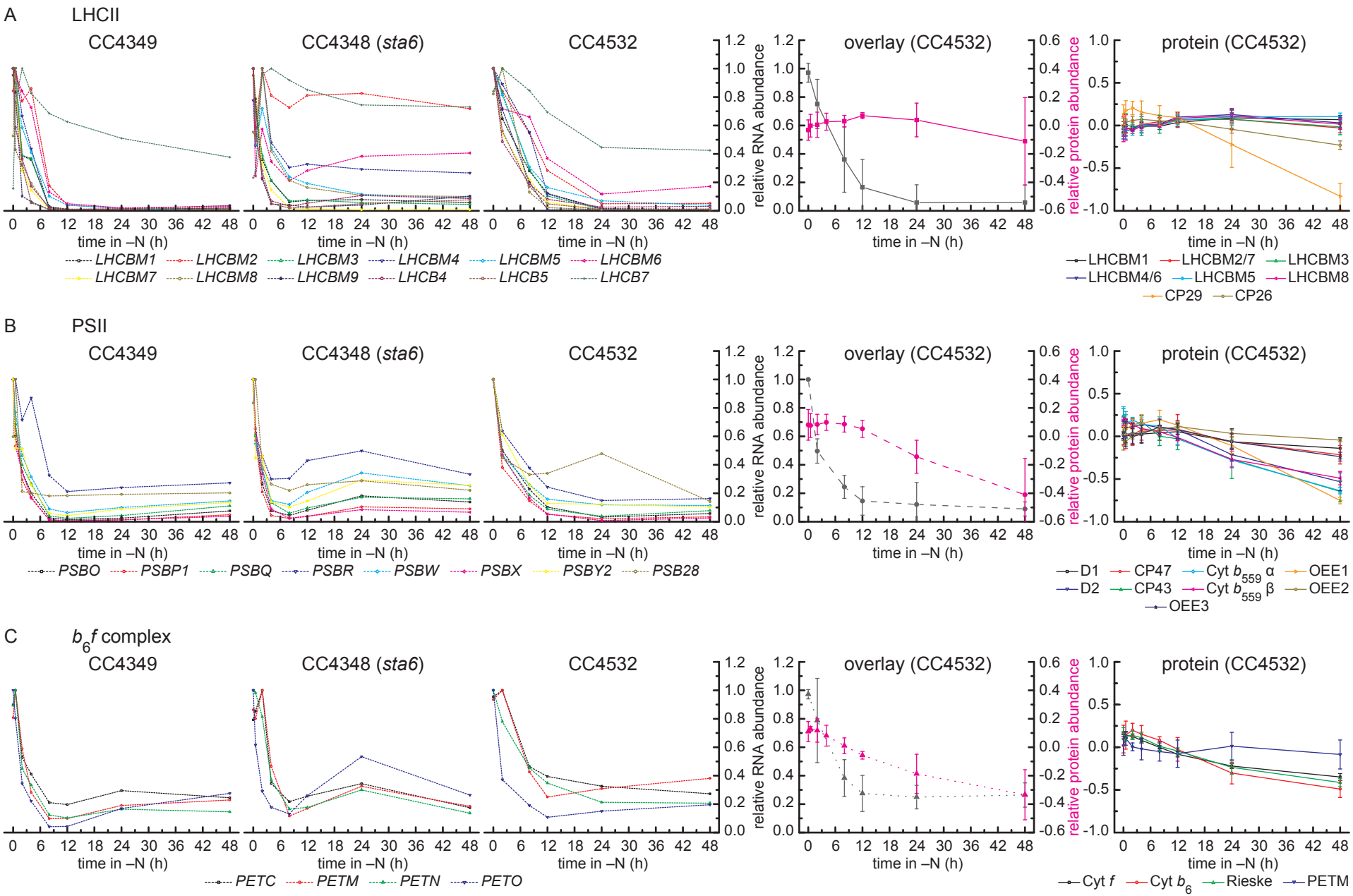

Supplemental Figure 5: mRNA and protein abundances for components of the photosynthetic complexes

mRNA and protein abundances are summarized for light harvesting complex II (A), photosystem II (B), cytochrome b_6f complex (C), light harvesting complex I (D), photosystem I (E) and plastidic ATP synthase (F).

Left: Relative mRNA abundance (% max) in Chlamydomonas strain CC4349, CC4348 (*sta6*) and CC4532 (48 h time course). See legend for individual gene names (left, italic). Cells were collected at the indicated time point after transfer to N-free medium, mRNA was purified and cDNA was generated for RNA-Seq analysis. Expression estimates of Au10.2 models are reported in units of RPKM (Mortazavi et al., 2008). The maximal RPKM was set to 1 to compare relative expression between individual genes.

Supplemental Figure 5: Photosynthesis - continued

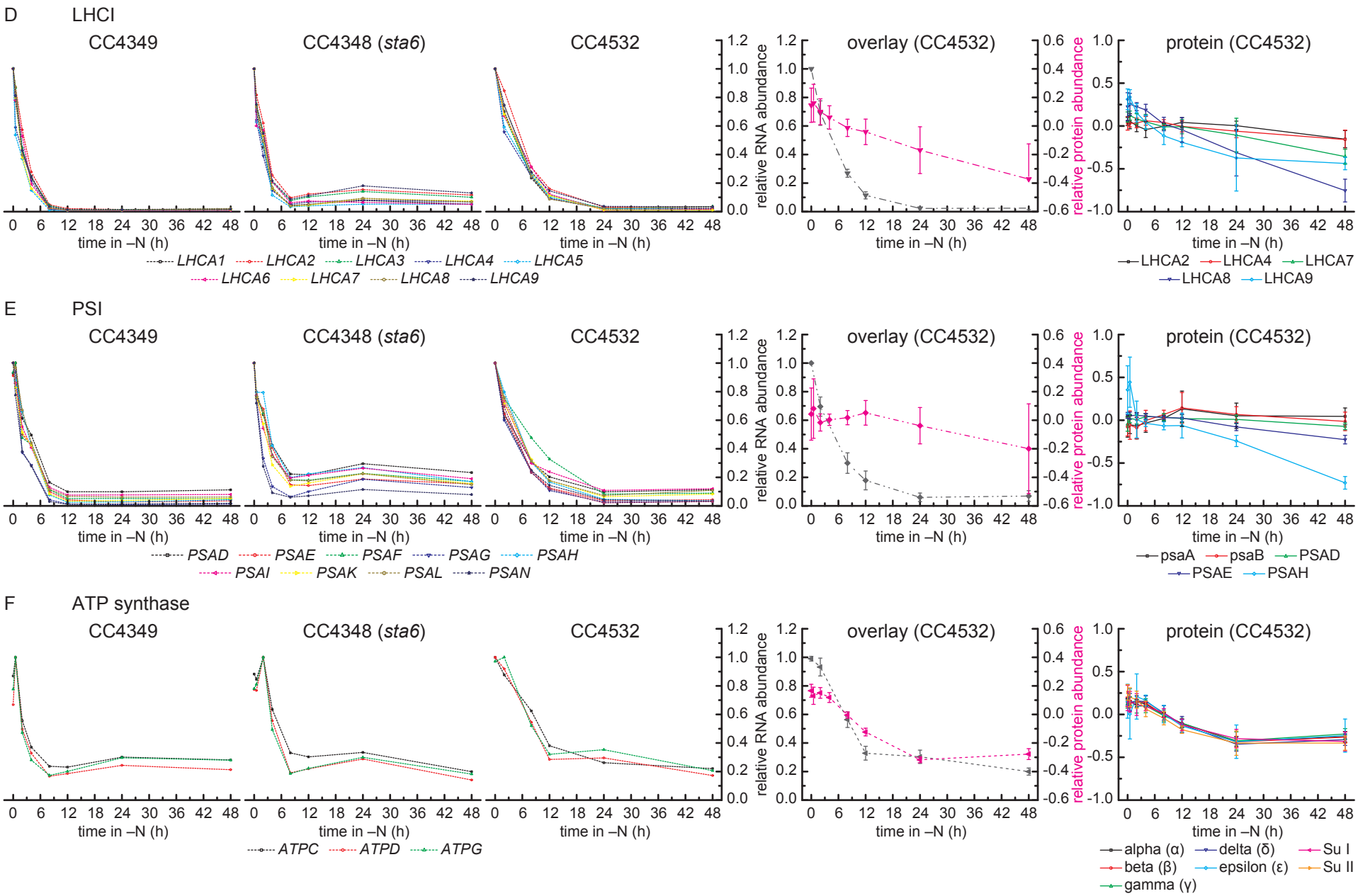

Supplemental Figure 5 - continued

Right: Abundance of proteins in each sample is compared to a ^{15}N labeled standard (see legend on the right for individual protein names). The $^{14}N/^{15}N$ ratio was obtained using quantitative LC-MS/MS analysis and is expressed here on a $\log_2$ transformed scale. Cells were collected at the indicated time point after transfer to nitrogen-free media.

Middle: Overlay of average relative abundance of mRNAs (grey) and proteins (pink) in Chlamydomonas strain CC4532, average protein abundances are drawn similar to Figure 2 in the main body to allow for comparison. Error bars indicate standard deviation between individual proteins/RNAs and lower case protein names on the right indicate origin from the plastid genome.

Supplemental Figure 6: Respiration

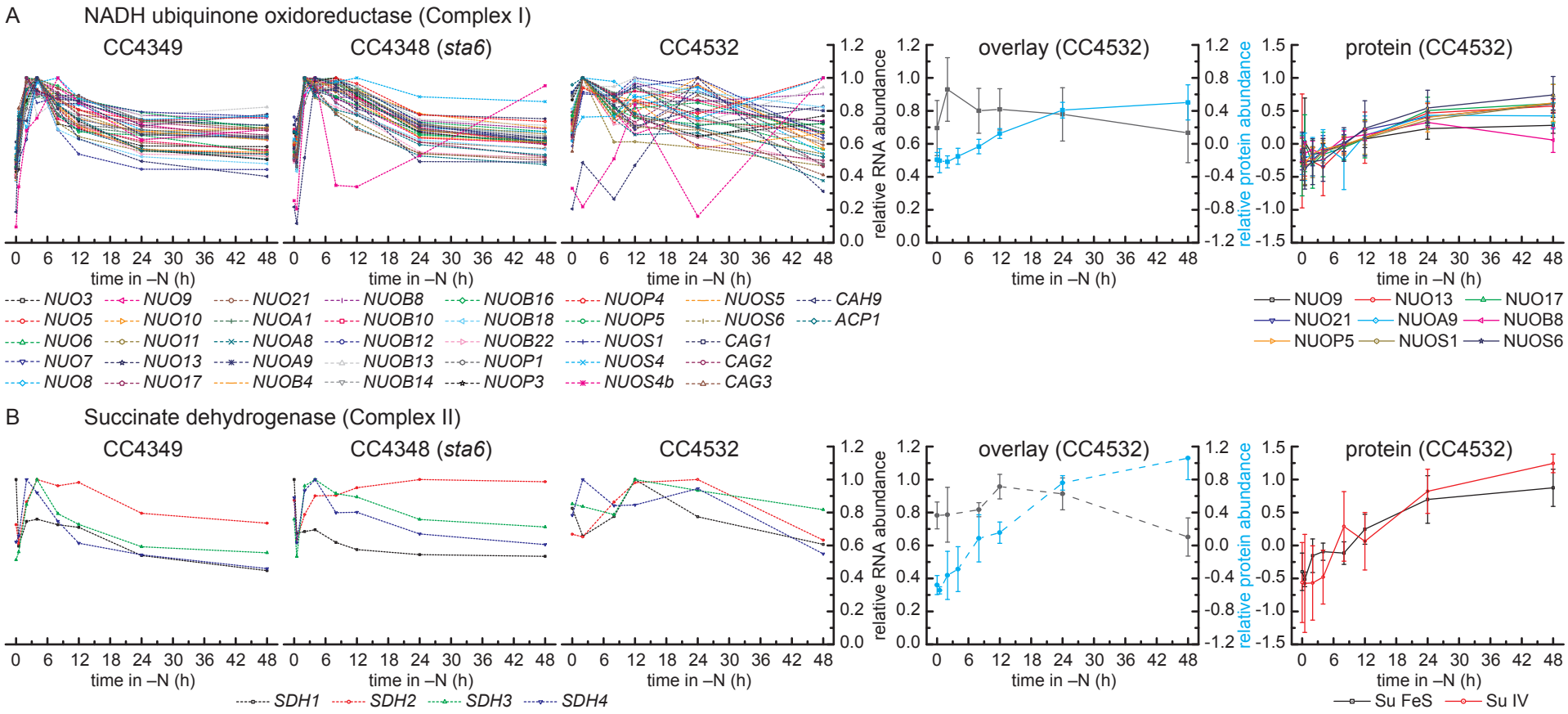

Supplemental Figure 6: mRNA and protein abundance of components of the respiratory complexes

Picture composed as described in Supplemental Figure 5 (see legends for individual gene/protein names). Average protein abundances for mitochondrial complexes are drawn in cyan similar to Figure 2 in the main body to allow for comparison. mRNA and protein abundances of NADH ubiquinone oxidoreductase (A, Complex I), succinate dehydrogenase (B, Complex II), ubiquinol cytochrome *c* oxidoreductase (C, Complex III), cytochrome *c* oxidase (D, Complex IV) and mitochondrial ATP synthase (E, Complex V).

Supplemental Figure 6: Respiration - continued

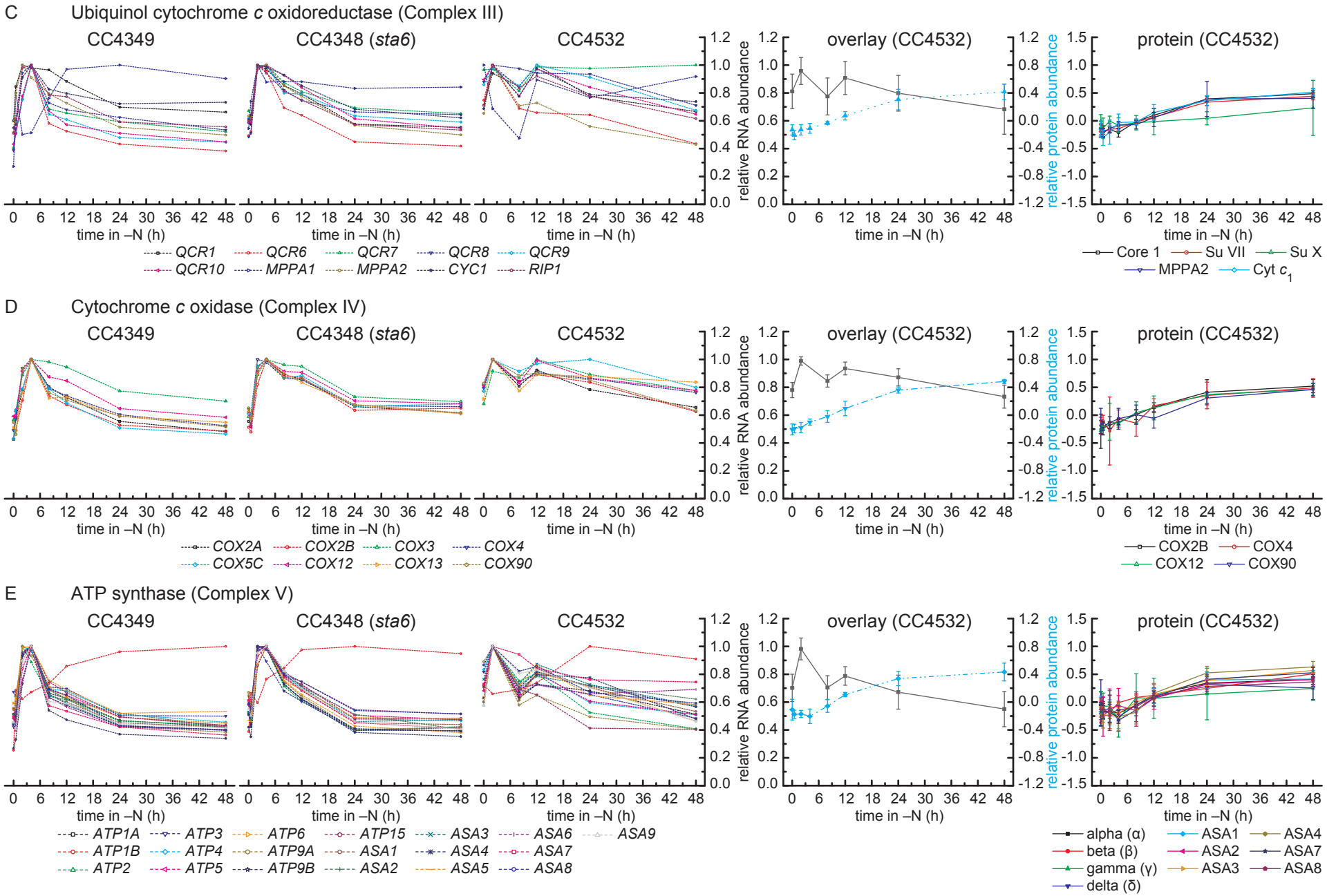

Supplemental Figure 7: Calvin-Benson cycle

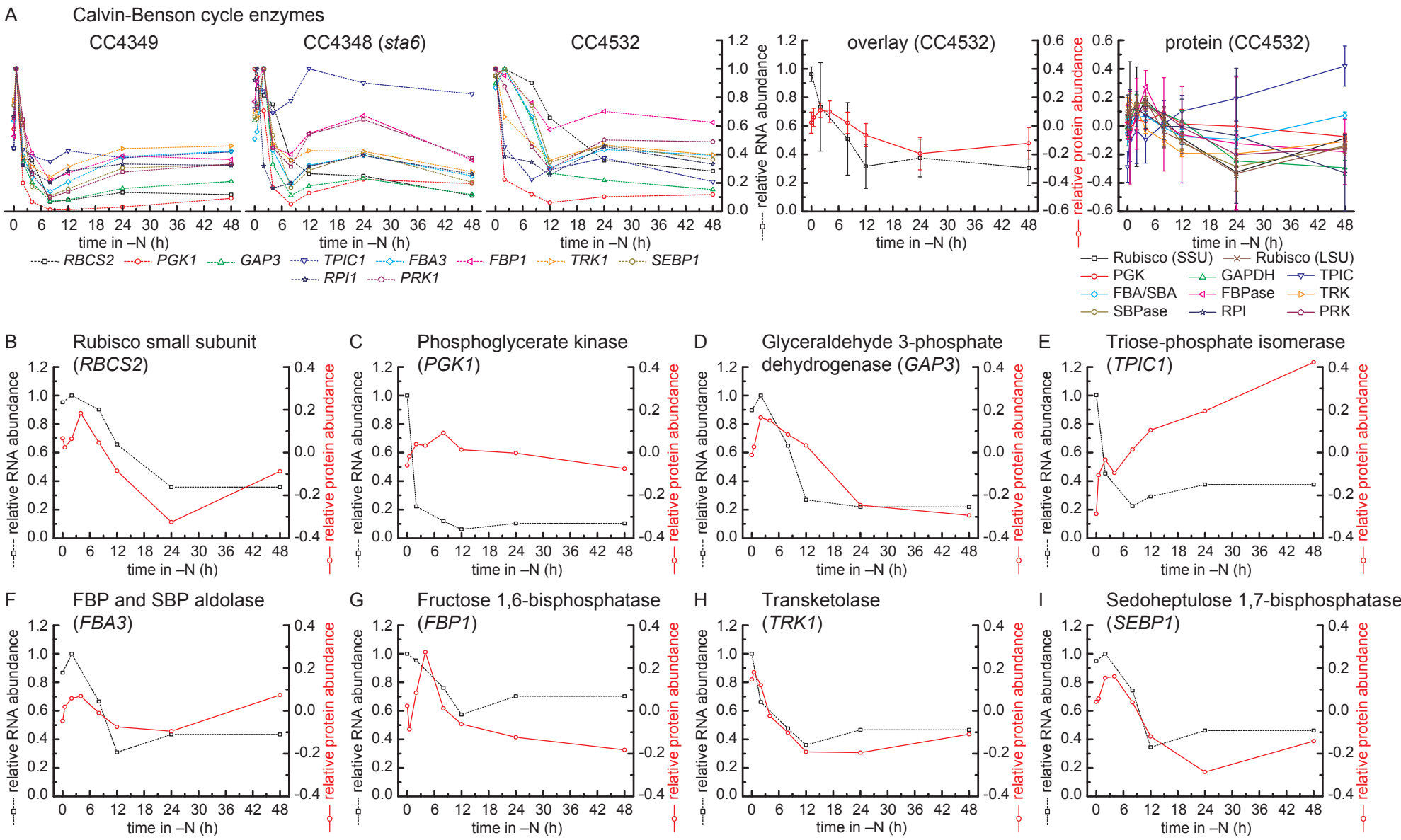

Supplemental Figure 7: mRNA and protein abundance of enzymes involved in Calvin-Benson cycle

Picture composed as described in Supplemental Figure 5 (see legends for individual gene/protein names). mRNA and protein abundance of all Calvin-Benson cycle enzymes (A) and overlays of each individual enzyme (B-L), as labelled. For each enzyme only the highest expressed potentially encoding gene and corresponding protein is shown.

Supplemental Figure 7: Calvin-Benson cycle - continued

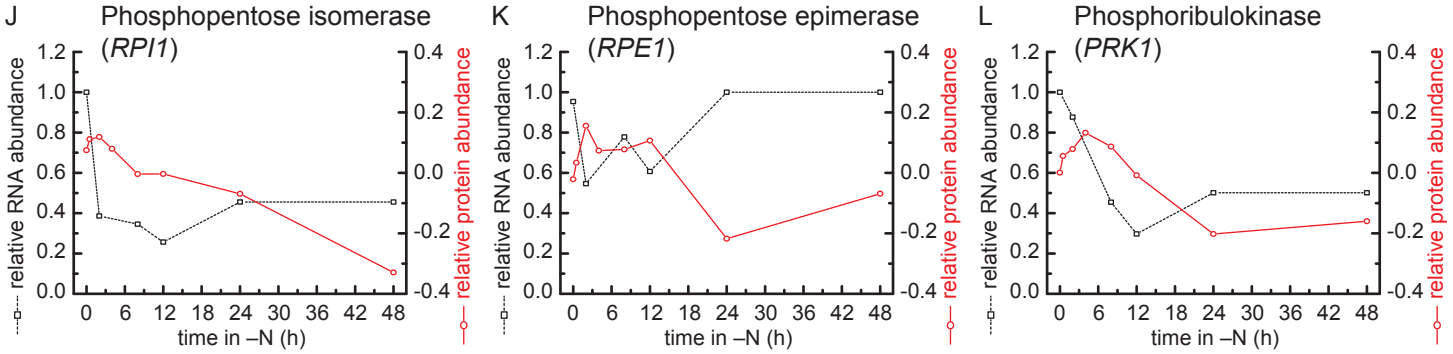

Supplemental Figure 8: Tetrapyrrole metabolism

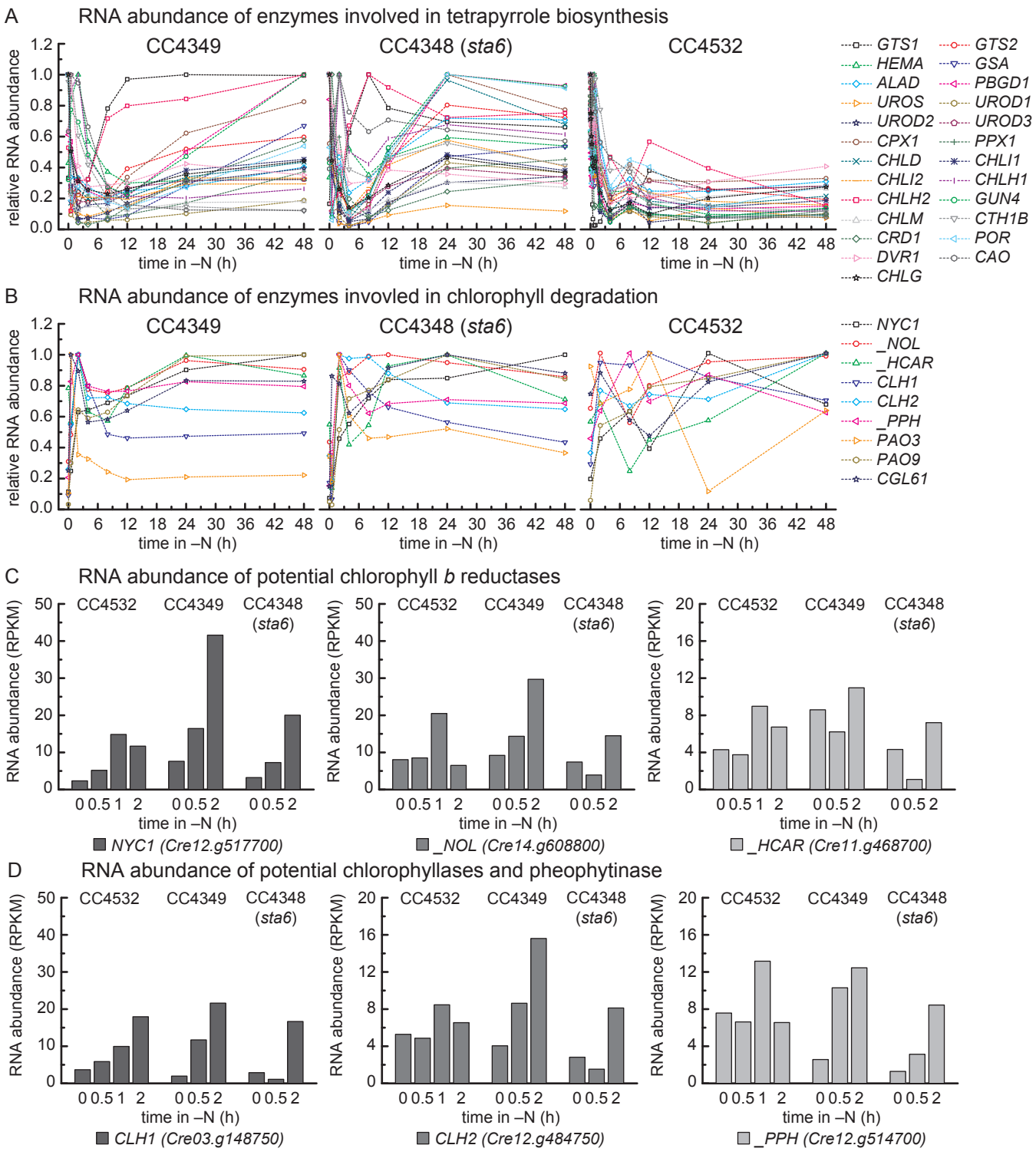

Supplemental Figure 8: mRNA abundances of enzymes involved in tetrapyrrole biosynthesis and degradation

Relative mRNA abundance (% max) of enzymes from tetrapyrrole metabolism in Chlamydomonas strain CC4349, CC4348 (*sta6*) and CC4532 (all experiments), see legends for individual gene names. mRNA was analyzed similar to what was described in Supplemental Figure 5. mRNA abundance of tetrapyrrole biosynthesis enzymes (A) and candidate RNAs potentially involved in chlorophyll degradation (B, 48 h experiment (L)). Absolute mRNA abundance (RPKM) from 0 to 2 h N deprivation in Chlamydomonas strain CC4532, CC4349 and CC4348 (*sta6*) is given for chlorophyll *b* reductases (C), chlorophyllases and pheophytinase (D), pheophorbide *a* oxygenases (E) and *CGL61* (F).

Supplemental Figure 8: Tetrapyrrole metabolism - continued

E RNA abundance of candidate pheophorbide *a* oxygenases

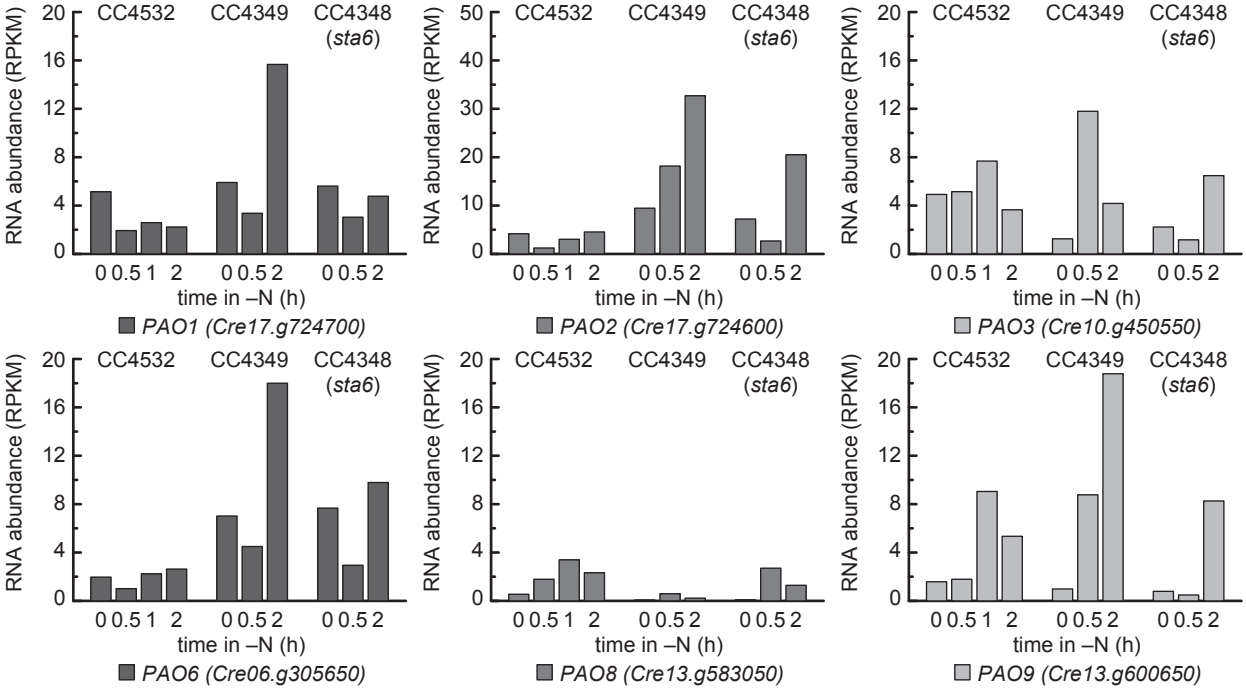

F RNA abundance of *CGL61*

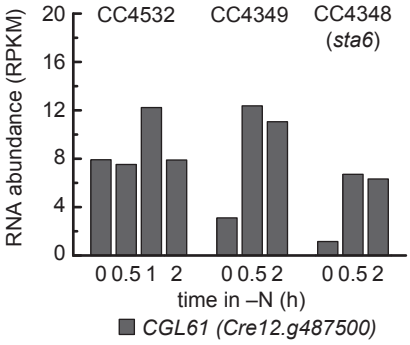

Supplemental Figure 9: Alignment of chlorophyll *b* reductases

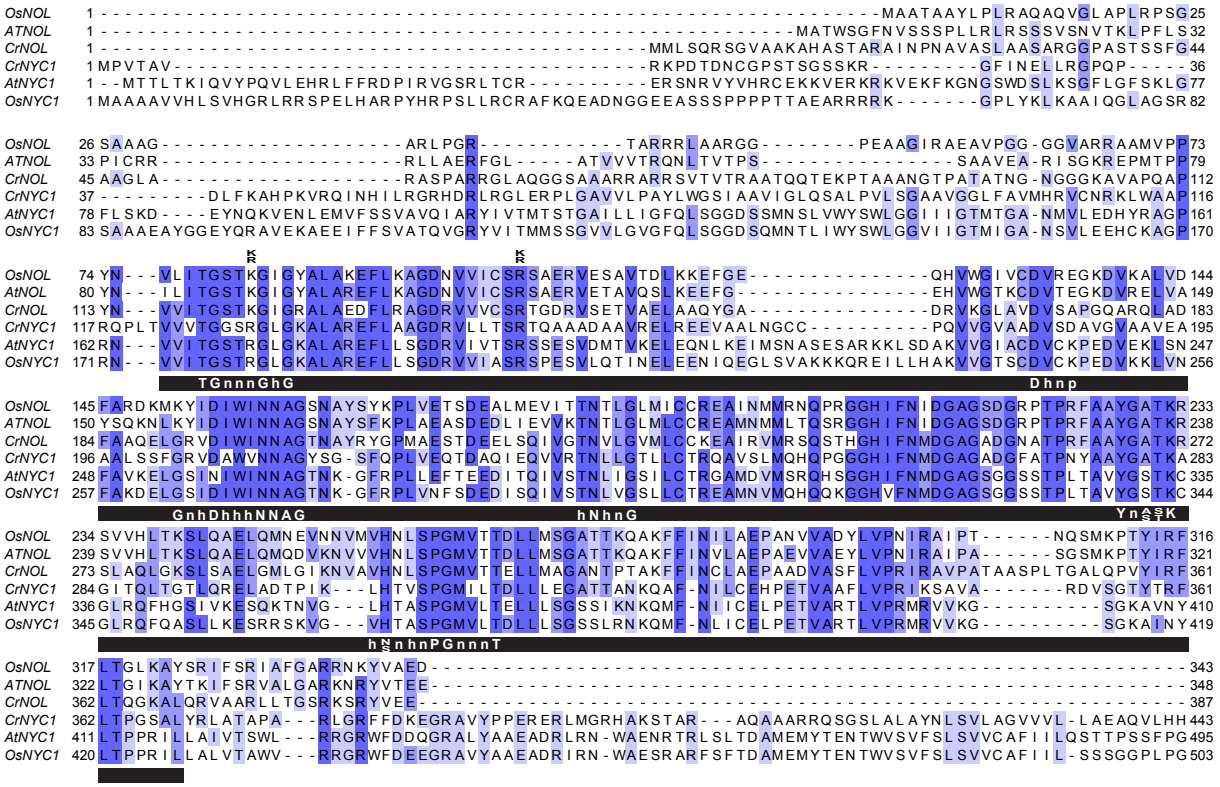

Supplemental Figure 9: Alignment of putative chlorophyll *b* reductases from *Oryza sativa*, *Arabidopsis thaliana* and *Chlamydomonas reinhardtii*

Amino acid sequences of NYC1 from *Oryza sativa* (Os-NYC1, GenBankID: BAF49740.1), its putative orthologs in *Arabidopsis thaliana* (At-NYC1, TAIR: AT4G13250) and *Chlamydomonas reinhardtii* (Cr-NYC1, Phytozome: Cre12.g517700) as well as the closely related chlorophyll *b* reductase NOL from rice (Os-NOL, GenBankID: BAF49741.1) and its putative orthologs At-NOL (AT5G04900) and Cr-NOL (Cre14.g608800) were aligned using the Muscle multiple alignment algorithm (Edgar, 2004) via the web service in Jalview software (version 2.8) (Waterhouse et al., 2009), which was also used for major editing. The sequences are ordered according to their MuscleWS similarity. Residues conserved in either 5 or 6 of the proteins are highlighted with a dark blue background, residues conserved in 3 or 4 of the proteins with a light blue background. Regions with high similarity to short-chain dehydrogenases identified using CDsearch (Marchler-Bauer and Bryant, 2004) are indicated with a black box, important sequence motifs conserved in short chain dehydrogenases are denoted in white bold letters (n = any amino acid, h = hydrophobic amino acid, p = polar or charged amino acid). The two positions indicative for the cofactor that is bound are denoted in black bold letters above the, NADPH is most likely the cofactor when both positions are either lysine or arginine (K/R) (Tanaka et al., 1996). Adobe Illustrator was used for the final editing.

Supplemental Figure 10: Heme biosynthesis and breakdown

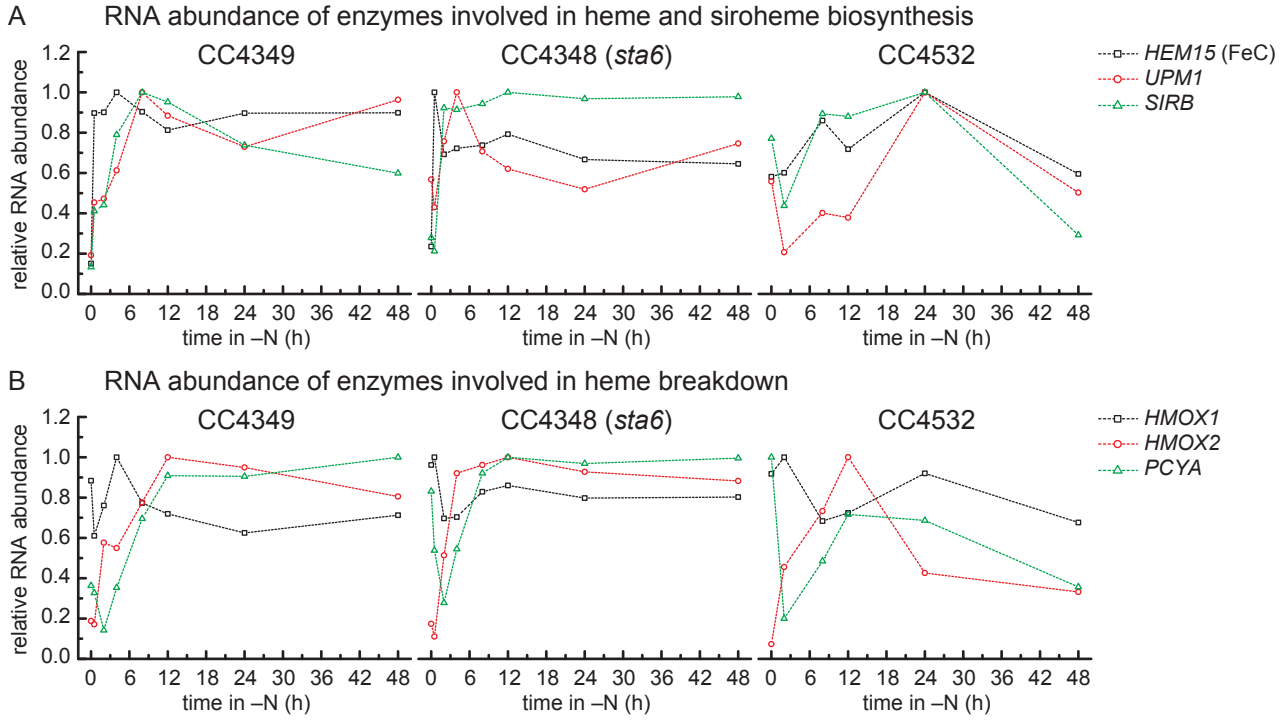

Supplemental Figure 10: mRNA abundance of enzymes involved in heme biosynthesis and degradation

Relative mRNA abundance (% max) of enzymes from heme metabolism in Chlamydomonas strain CC4349, CC4348 (*sta6*) and CC4532 (48 h experiment), see legends for individual gene names. mRNA was analyzed similar to what was described in Supplemental Figure 5. mRNA abundance of enzymes involved in heme and siroheme biosynthesis (A) and enzymes involved in heme degradation (B).

Supplemental Figure 11: Ribosomes - chloroplast

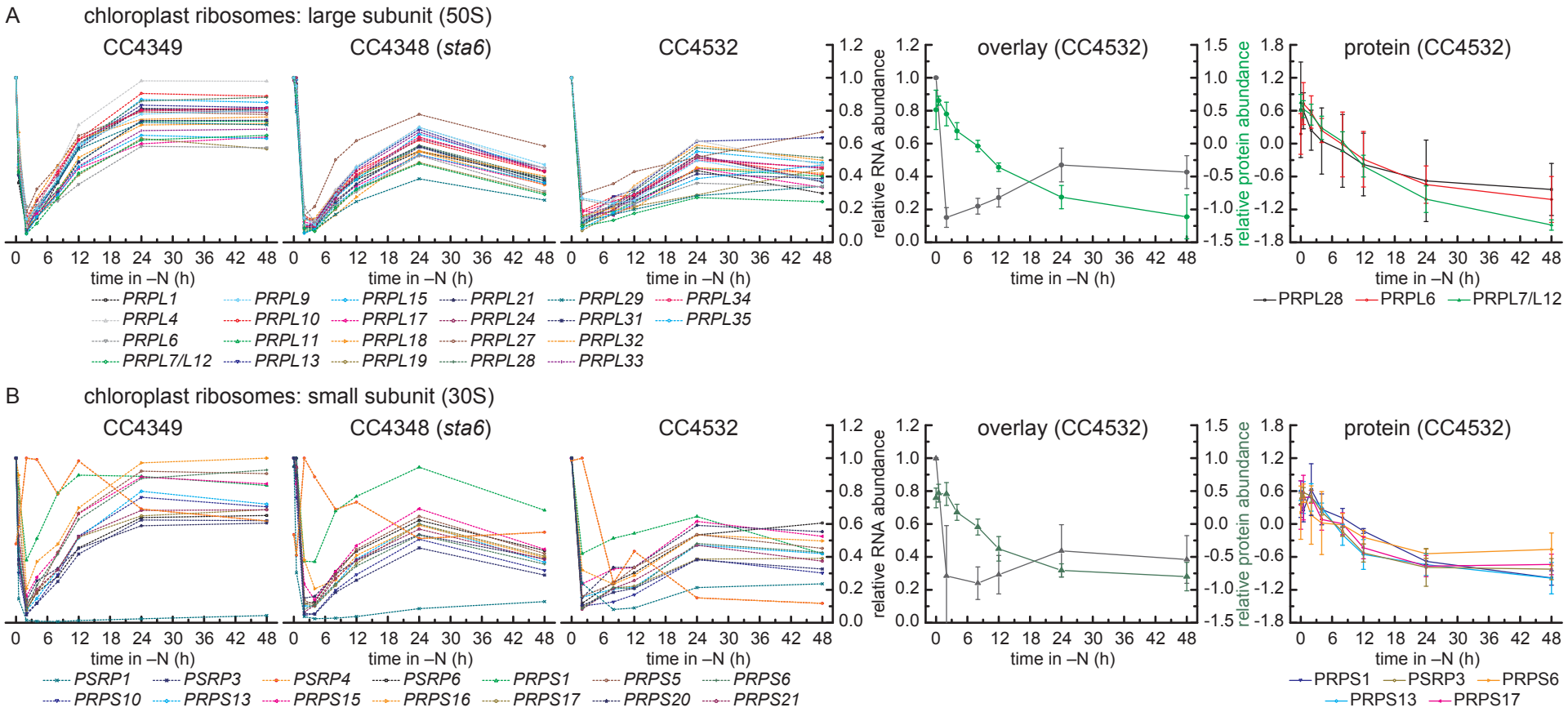

Supplemental Figure 11: Abundance of ribosomal proteins and corresponding mRNAs

Picture composed as described in Supplemental Figure 5 (see legends for individual gene/protein names). Average protein abundances of cytosolic/plastidic complexes are drawn similar to Figure 6 in the main body to allow for comparison. mRNA and protein abundances of chloroplast ribosomal proteins from the large 50S subunit (A) and small 30S subunit (B) as well as cytosolic ribosomal proteins from the large 60S subunit (C) and small 40S subunit (D). For mitochondrial ribosomal proteins mRNA abundance of the large 50S subunit (E) and small 30S subunit (F) is summarized.

Supplemental Figure 11: Ribosomes - cytosol

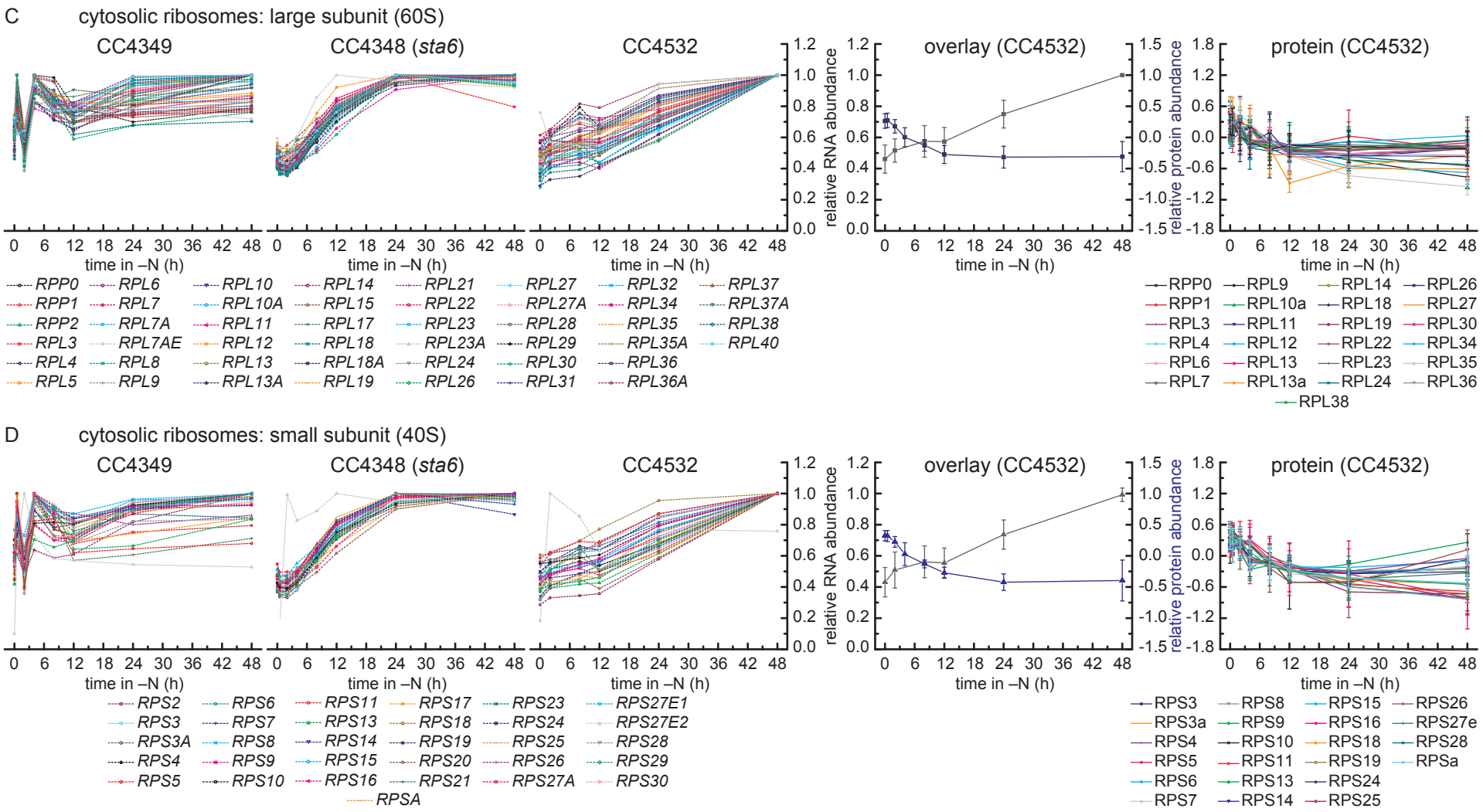

Supplemental Figure 11: Ribosomes - mitochondria

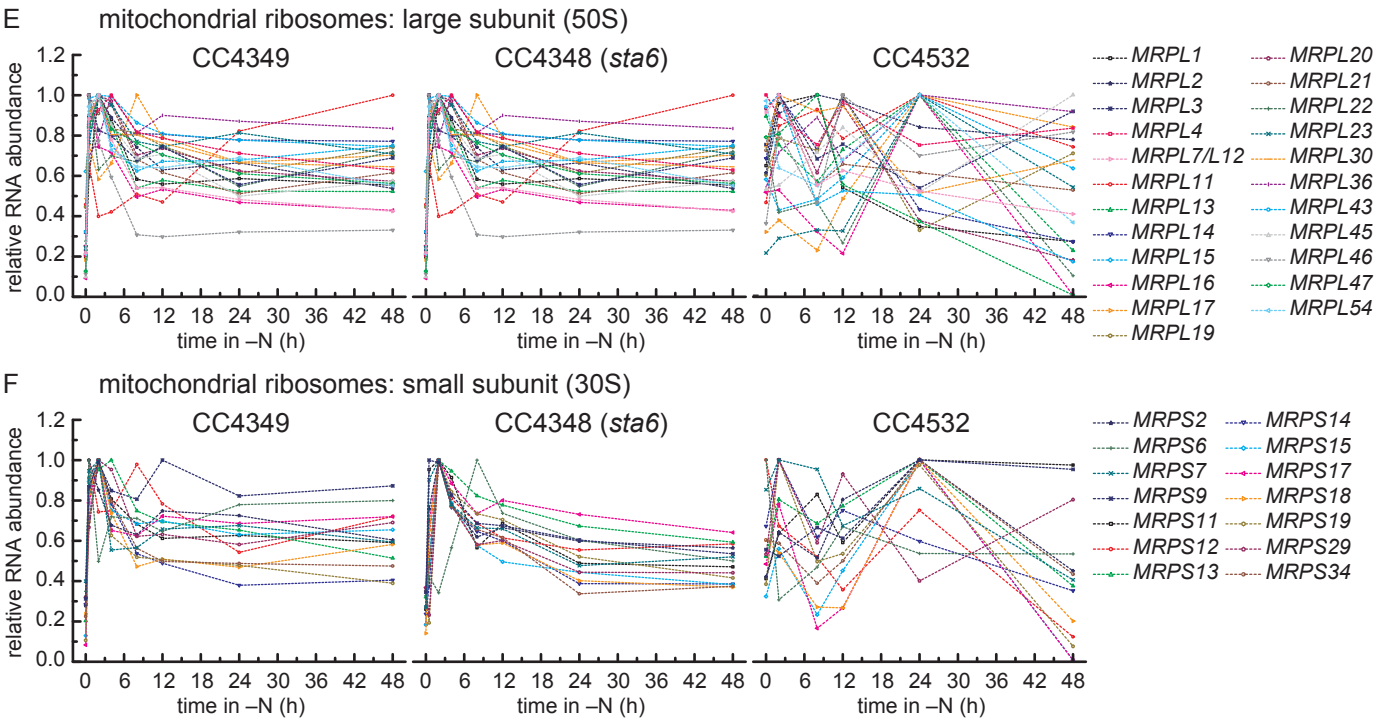

Supplemental Figure 12: N Sparing

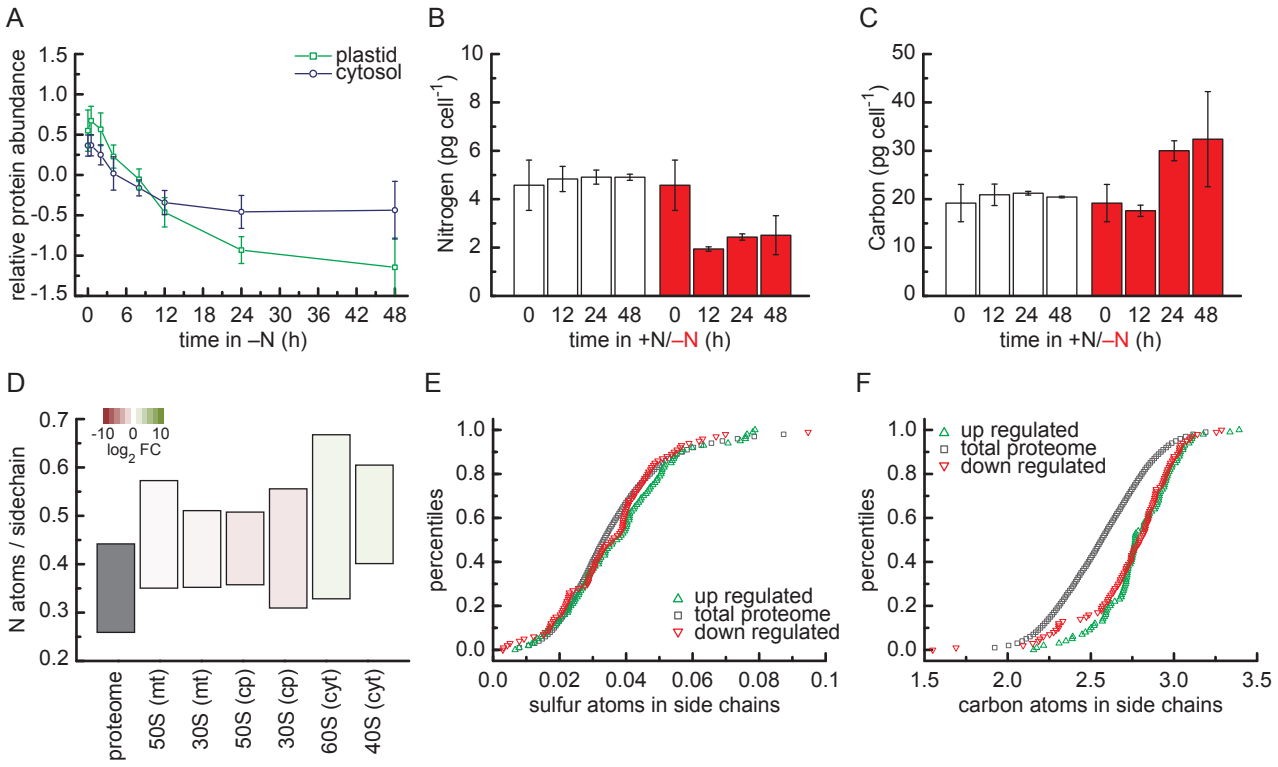

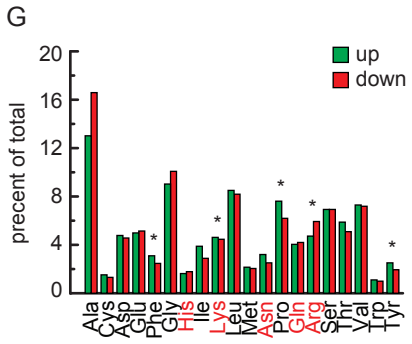

Supplemental Figure 12: Nitrogen sparing mechanisms in Chlamydomonas

A: Overlay of cytosolic and chloroplast ribosomal average protein abundance: Relative protein abundance compared to a ^{15}N labeled standard ($^{14}N/^{15}N$ ratio) for each measured protein was averaged for cytosolic ribosomal proteins (blue) and chloroplast ribosomal proteins (green). Error bars indicate standard deviation between individual proteins.

B: Total nitrogen content: Nitrogen content (pg/cell) at the indicated time points after transfer to N-free medium measured on a TOC/TN analyzer. Error bars indicate standard deviation of three independent biological replicates.

C: Total non-purgeable organic carbon content: Carbon content (pg/cell) at the indicated time points measured on a TOC/TN analyzer. Error bars indicate standard deviation of three independent biological replicates.

D: Nitrogen content of ribosomal proteins: Range (10% quantile (Q_{10}) to 90% quantile (Q_{90})) of average number of nitrogen atoms in amino acid side chains in the proteome and in ribosomal proteins from different compartments. Color indicates (average) $\log_2$ fold change of mRNA abundance (green increase, red decrease) within 48 h of nitrogen deprivation in Chlamydomonas strain CC4532. Nitrogen content in side chains is based on Augustus 10.2 gene models.

E: Comparison of sulfur content between up and down-regulated proteins: Quantile distributions of sulfur atoms in amino acid side chains of up (green) or down-regulated (red) proteins. The whole proteome based on Augustus 10.2 gene models was used for reference (grey).

F: Comparison of carbon content between up and down-regulated proteins: Picture composed as described in E for distributions of carbon atoms in amino acid side chains.

G: Amino acid composition in increasing and decreasing proteins within the proteome: The distributions of the individual amino acids within the proteomics data set is shown, divided into accumulating (up, green) or decreasing (down) proteins upon N starvation. In each data series the total count is normalized to 1. Asterisks indicate statistical significance (t-test, p-value < 0.05) in the differences between the set of accumulating proteins or decreasing proteins (at 48 h time point).

Supplemental Figure 13: Autophagy

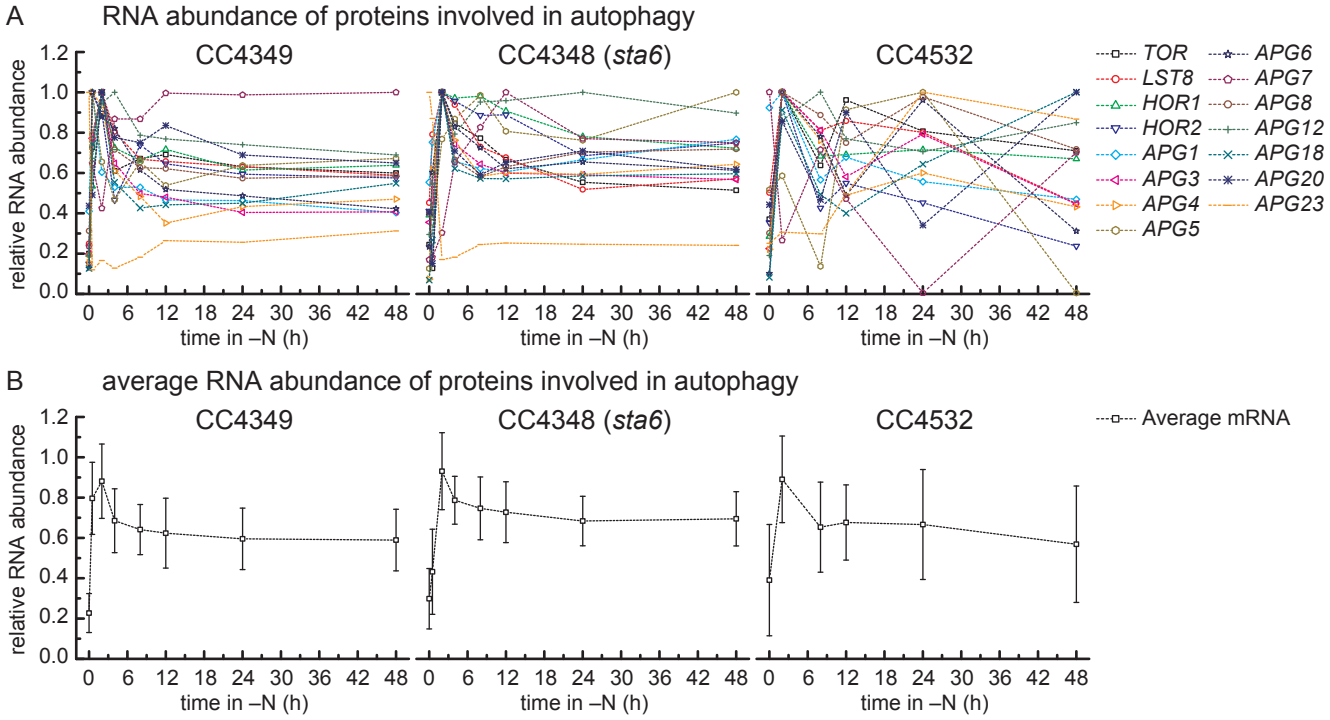

Supplemental Figure 13: Abundance of autophagy-related genes

A: mRNA abundance of genes involved in autophagy: Relative mRNA abundance (% max) for proteins involved in autophagy in Chlamydomonas strain CC4349, CC4348 (*sta6*) and CC4532 (48 h time course). mRNA was analyzed similar to what was already described in Supplemental Figure 5. See legend for individual gene names. The gene list derived from (Díaz-Troya et al., 2008).

B: Average mRNA abundance of genes involved in autophagy: mRNA from genes in A was averaged, error bars indicate standard deviation between individual genes.

Supplemental Figure 14

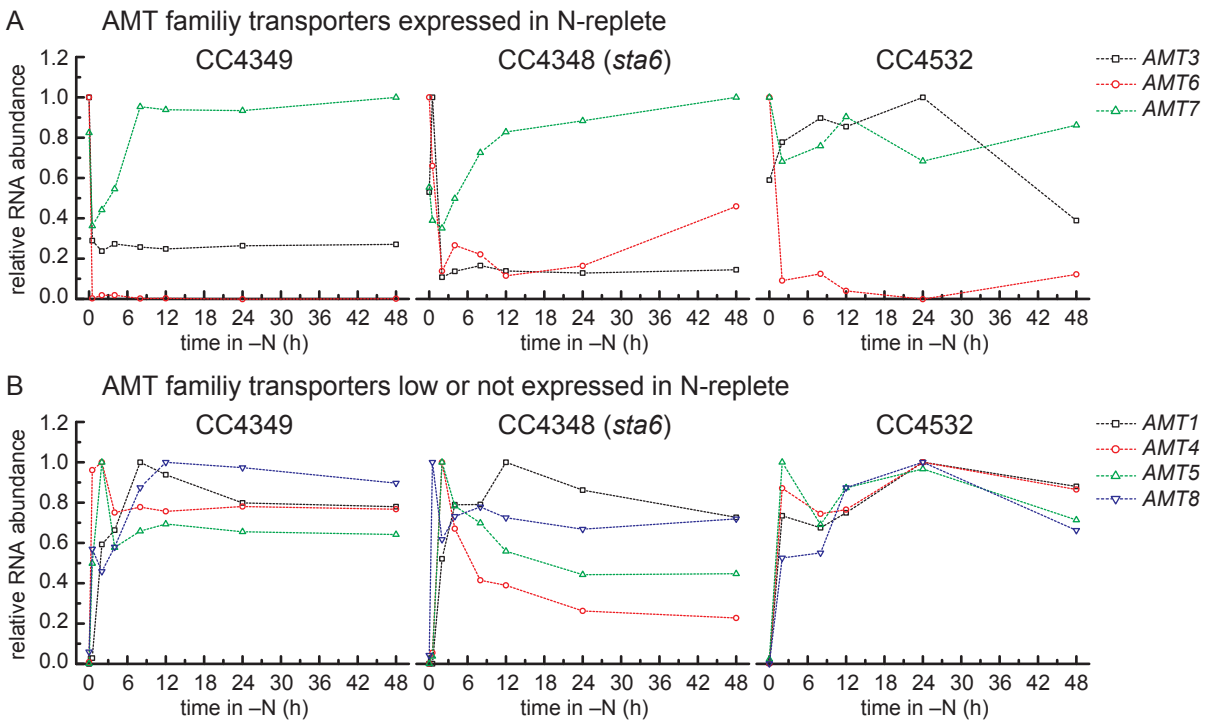

Supplemental Figure 14: mRNA abundance of transporters involved in ammonium import

Relative mRNA abundance (% max) of NH_4^+ transporters from the AMT family in Chlamydomonas strain CC4349, CC4348 (*sta6*) and CC4532 (48 h experiment), see legends for individual gene names. mRNA was analyzed similar to what was described in Supplemental Figure 5. mRNA abundance of AMT transporters present in N-replete (A) and absent or very low expressed in N-replete (B).

Supplemental Figure 15

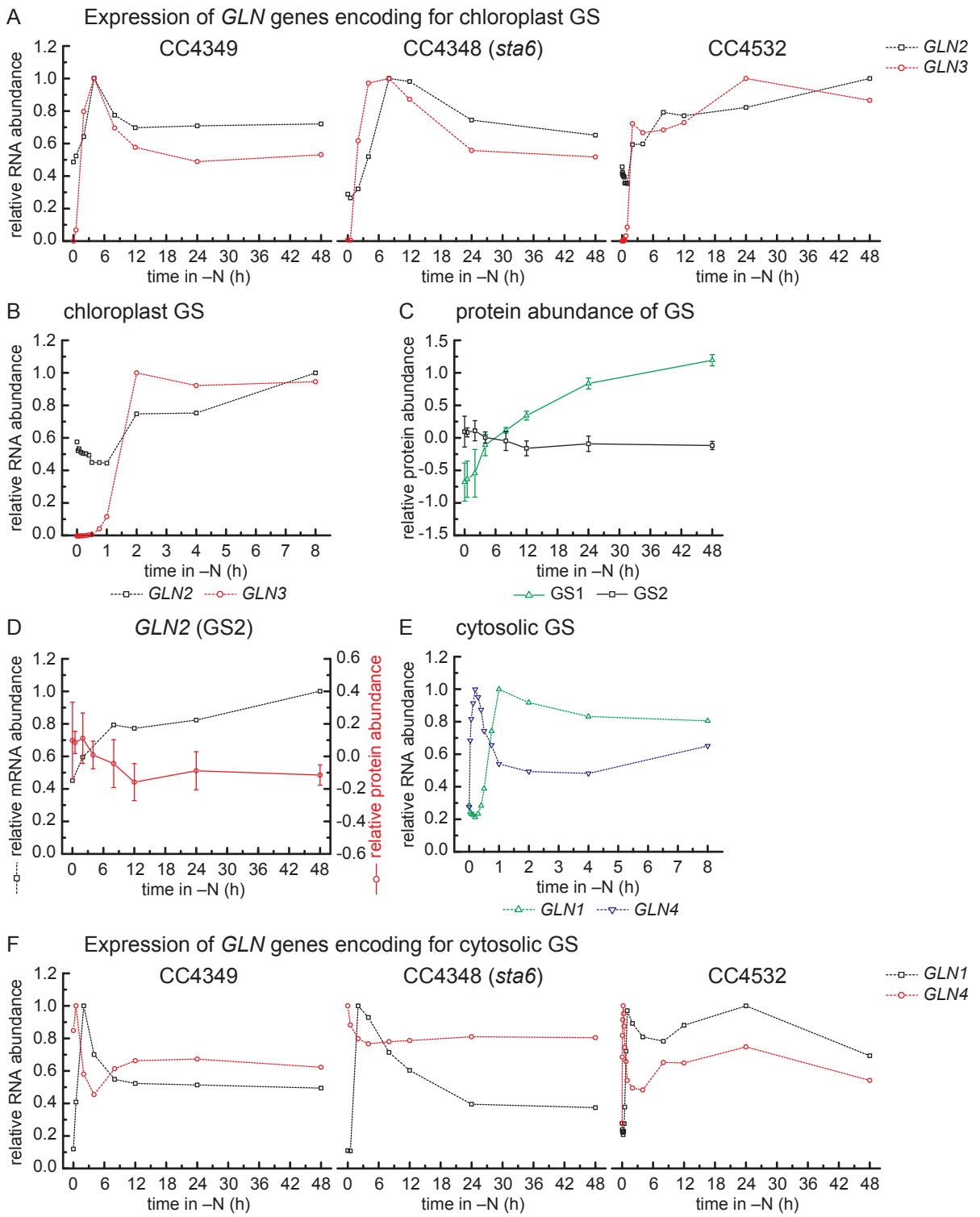

Supplemental Figure 15: Abundance of glutamine synthases (GS) and *GLN* RNAs

A and B: Relative abundance of *GLN* RNAs encoding plastidic GS enzymes: Relative abundance (% max) of *GLN2* and *GLN3* upon transfer to N-free media (A, 48 h) in Chlamydomonas strain CC4349, CC4348 (*sta6*) and CC4532 (all experiments) and within the first 8 h of N deprivation in Chlamydomonas strain CC4532 (B, 1 h and 8 h experiment). mRNA was analyzed similar to what was already described in Supplemental Figure 5.

C: Abundance of cytosolic and chloroplast GS: Relative protein abundances compared to a ^{15}N labeled standard ($^{14}N/^{15}N$ ratio) for GS as described in Supplemental Figure 5. Error bars indicate standard deviation between individual experiements.

D: Overlay of protein and mRNA abundance of GS2 (*GLN2*): The relative abundance of *GLN2* mRNA (% max) within the 48 h N deprivation experiment (L) in Chlamydomonas strain CC4532 is displayed in grey. The relative abundance ($^{14}N/^{15}N$, $\log_2$ transformed) for the GS2 protein is given in red.

E and F: Relative abundance of *GLN* RNAs encoding cytosolic GS enzymes: Relative abundance (% max) of *GLN1* and *GLN4* upon transfer to N-free media (E, 48 h) in Chlamydomonas strain CC4349, CC4348 (*sta6*) and CC4532 (all experiments) and within the first 8 h of N deprivation in Chlamydomonas strain CC4532 (F, 1 h and 8 h experiment). mRNA was analyzed similar to what was already described in Supplemental Figure 5.

Supplemental Figure 16: RNA and protein abundance of GOGAT enzymes

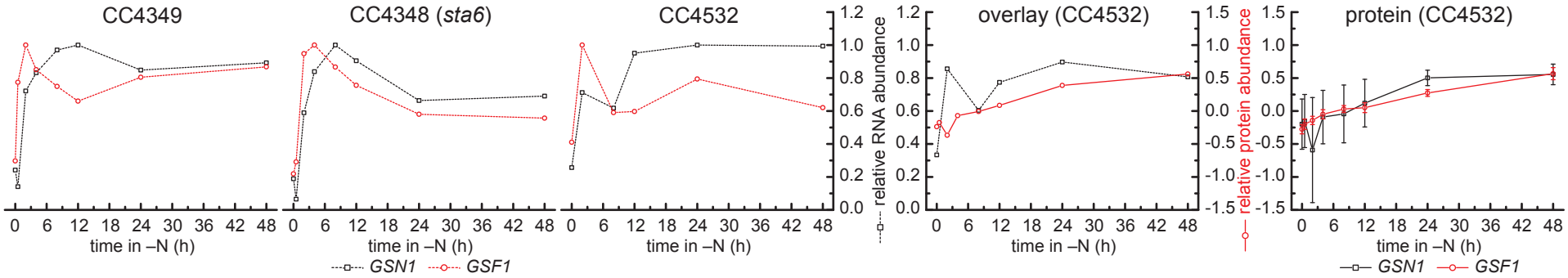

Supplemental Figure 16: Abundance of glutamate oxoglutarate amidotransferases (GOGAT) and corresponding mRNAs
Picture composed as described in Supplemental Figure 5 (see legends for individual gene/protein names).

Supplemental Figure 17

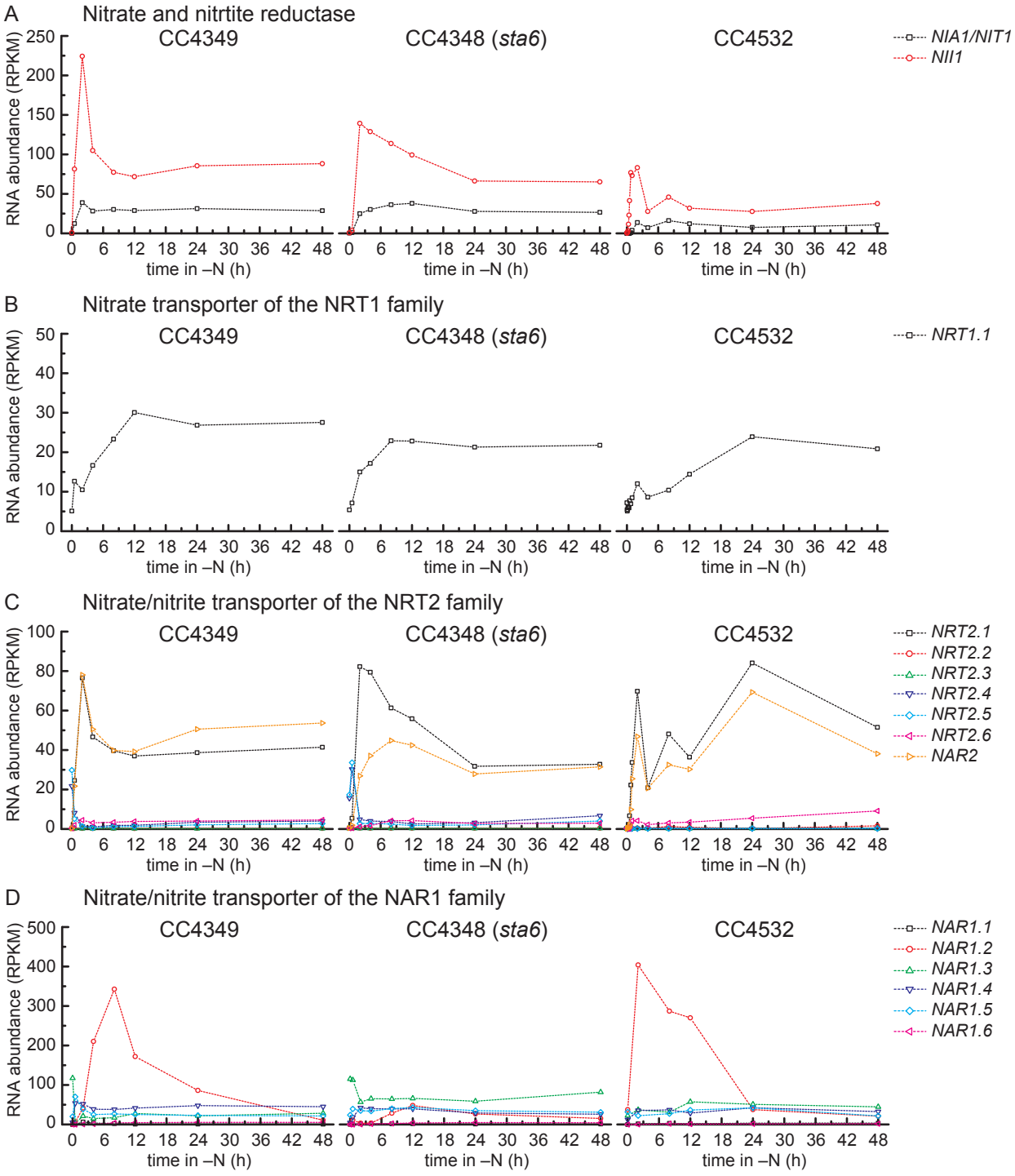

Supplemental Figure 17: Abundance of RNAs encoding nitrate or nitrite metabolism functions

mRNA abundance (RPKM) of proteins involved in NO_3/NO_2 assimilation in Chlamydomonas strain CC4349, CC4348 (*sta6*) and CC4532 (all experiments), see legends for individual gene names. mRNA was analyzed similar to what was described in Supplemental Figure 5. mRNA abundance of nitrate (NR) and nitrite reductase (NiR) (A), nitrate transporters of the NRT1 family (B), nitrate/nitrite transporters of the NRT2 family (C) and nitrite transporters from the NAR1 family (D) upon transfer to N-free media.

Supplemental Figure 18

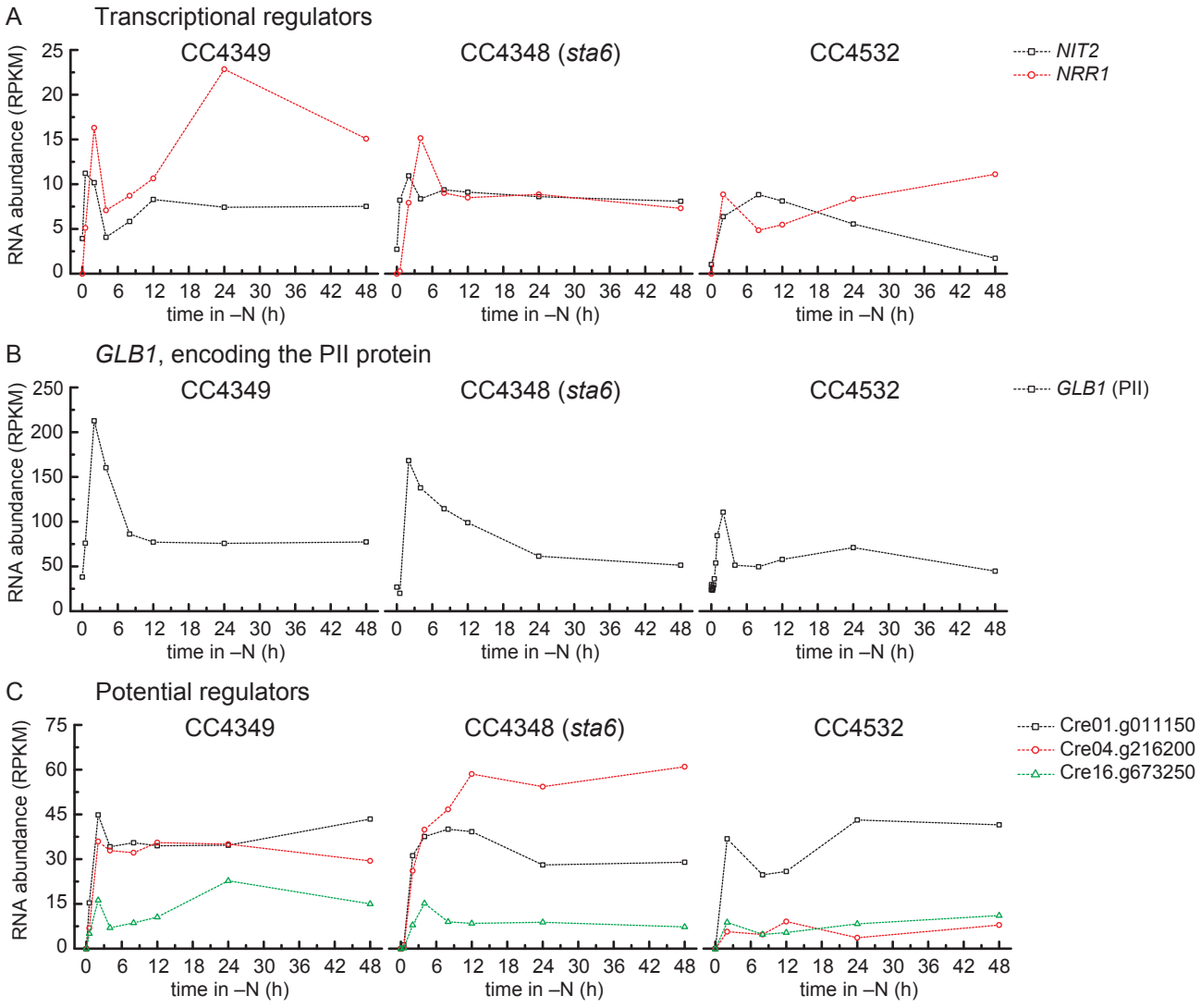

Supplemental Figure 18: Abundance of RNAs encoding (potential) regulators of N assimilation

mRNA abundance (RPKM) of proteins (potentially) regulating N assimilation in Chlamydomonas strain CC4349, CC4348 (*sta6*) and CC4532 (48 h experiment), see legends for individual gene names. mRNA was analyzed similar to what was described in Supplemental Figure 5. mRNA abundance of *NIT2* and *NRR1* (A), the *GLB1* gene encoding the PII protein (B) and three co-regulated transcription factors from Cluster 25 (C) upon transfer to N-free media. N content within side chains is provided for the characterized and potential transcriptional regulators (D). Range (from the 10 % to 90 % quantile) of average number of nitrogen atoms in amino acid side chains in all proteins of the proteome and in all transcription factors as proposed from either Perez-Rodriguez et al. 2010 or Zhang *et al.* 2011. The color indicates (average) $\log_2$ fold changes of mRNA abundance (green - increase, red - decrease) between N-replete conditions and 60 min after the transfer to N-free medium in Chlamydomonas strain CC4532. The nitrogen content in side chains is based on Augustus 10.2 gene models.

Supplemental Table 1: Overlap of differentially accumulating mRNAs between all and individual strains

Comparison of all three strains	Chlamydomonas strain		
	CC4532	CC4349	CC4348 (*sta6*)
total DE[1] genes (No.)	4288	8482	8200
unique (No.)	579	1434	1221
unique (%)	0.135	0.169	0.149
conserved in all strains (No.)	2914	2914	2914
conserved in all strains (%)	0.680	0.344	0.355
add. overlap only with CC4349 (No.)	432	-	3702
add. overlap only with CC4349 (%)	0.101	-	0.451
add. overlap only with CC4348 (*sta6*) (No.)	363	3702	-
add. overlap only with CC4348 (*sta6*) (%)	0.085	0.436	-
add. overlap only with CC4532 (No.)	-	432	363
add. overlap only with CC4532 (%)	-	0.051	0.044

Pairwise comparison	Chlamydomonas strain		
	CC4532	CC4349	CC4348 (*sta6*)
CC4532 (No.)	4288	3346	3277
CC4532 (%)	1	0.394	0.400
CC4349 (No.)	3346	8482	6616
CC4349 (%)	0.780	1	0.807
CC4348 (*sta6*) (No.)	3277	6616	8200
CC4348 (*sta6*) (%)	0.764	0.780	1

[1] differentially expressed according to statistical analysis summarized in Materials and Methods

Supplemental Table 2: Common patterns of changing mRNA abundances in nitrogen, sulfur and phosphorus deprivation

Comparison		No. of genes similar in CC4532 at each time point in N-free media (h)														
		0.03	**0.07**	**0.13**	**0.2**	**0.3**	**0.4**	**0.5**	**0.75**	**1**	**2**	**4**	**8**	**12**	**24**	**48**
-S/-N	**up/up**	42	52	62	78	99	114	133	165	168	153	167	173	162	167	157
	down/down	23	48	45	116	187	239	262	280	266	301	285	322	279	279	281
	ratio (up/down)	1.83	1.08	1.38	0.67	0.53	0.48	0.51	0.59	0.63	0.51	0.59	0.54	0.58	0.60	0.56
	up/down	9	20	15	14	18	17	16	10	12	8	5	7	5	6	6
	down/up	5	7	9	10	14	17	18	15	14	15	97	64	25	7	3
	similar	65	100	107	194	286	353	395	445	434	454	452	495	441	446	438
	opposite	14	27	24	24	32	34	34	25	26	23	102	71	30	13	9
	ratio (similar/opposite)	4.64	3.70	4.46	8.08	8.94	10.38	11.62	17.80	16.69	19.74	4.43	6.97	14.70	34.31	48.67
-P/-N	**up/up**	21	25	30	37	46	53	57	68	70	72	77	82	81	78	72
	down/down	0	0	0	2	13	21	28	39	38	41	39	45	41	39	40
	ratio (up/down)	N/A	N/A	N/A	18.50	3.54	2.52	2.04	1.74	1.84	1.76	1.97	1.82	1.98	2.00	1.80
	up/down	10	10	8	11	14	15	16	14	11	8	2	7	3	5	6
	down/up	2	2	1	1	1	0	0	0	0	0	1	0	0	1	0
	similar	21	25	30	39	59	74	85	107	108	113	116	127	122	117	112
	opposite	12	12	9	12	15	15	16	14	11	8	3	7	3	6	6
	ratio (similar/opposite)	1.75	2.08	3.33	3.25	3.93	4.93	5.31	7.64	9.82	14.13	38.67	18.14	40.67	19.50	18.67
-S/-P/-N	**up/up/up**	12	12	14	18	25	30	30	36	39	39	41	40	40	41	40
	down/down/down	0	0	0	2	10	17	24	33	34	38	38	42	40	38	40
	ratio (up/down)	N/A	N/A	N/A	9.00	2.50	1.76	1.25	1.09	1.15	1.03	1.08	0.95	1.00	1.08	1.00
	up/up/down	1	3	0	0	3	4	4	2	1	3	1	2	1	1	0
	up/down/up	0	0	0	0	0	0	0	0	0	0	0	0	0	0	0
	down/up/up	0	0	0	0	1	1	1	1	1	2	4	3	2	1	1
	down/down/up	0	0	0	0	0	0	0	0	0	0	0	0	0	0	0
	down/up/down	2	3	3	2	2	3	3	3	2	0	0	0	0	1	2
	up/down/down	0	0	0	0	0	0	0	0	0	0	0	0	0	0	0
	similar	12	12	14	20	35	47	54	69	73	77	79	82	80	79	80
	opposite	3	6	3	2	6	8	8	6	4	5	5	5	3	3	3
	ratio (similar/opposite)	4.00	2.00	4.67	10.00	5.83	5.88	6.75	11.50	18.25	15.40	15.80	16.40	26.67	26.33	26.67

Supplemental Table 2 - continued

Comparison		No. of genes similar in CC4349 at each time point in N-free media (h)						
		0.5	2	4	8	12	24	48
-S/-N	up/up	124	150	157	163	158	159	159
	down/down	156	277	218	176	121	119	142
	ratio (up/down)	0.79	0.54	0.72	0.93	1.31	1.34	1.12
	up/down	37	35	30	22	15	20	20
	down/up	91	90	92	89	80	74	72
	similar	280	427	375	339	279	278	301
	opposite	128	125	122	111	95	94	92
	ratio (similar/opposite)	2.19	3.42	3.07	3.05	2.94	2.96	3.27
-P/-N	up/up	66	79	84	88	88	87	85
	down/down	32	44	43	39	26	21	20
	ratio (up/down)	2.06	1.80	1.95	2.26	3.38	4.14	4.25
	up/down	12	14	10	6	5	8	6
	down/up	3	1	1	2	3	4	3
	similar	98	123	127	127	114	108	105
	opposite	15	15	11	8	8	12	9
	ratio (similar/opposite)	6.53	8.20	11.55	15.88	14.25	9.00	11.67
-S/-P/-N	up/up/up	36	43	43	44	44	44	44
	down/down/down	26	39	38	34	21	16	15
	ratio (up/down)	1.38	1.10	1.13	1.29	2.10	2.75	2.93
	up/up/down	3	3	2	0	0	1	0
	up/down/up	0	0	0	0	0	0	0
	down/up/up	3	4	4	4	4	4	4
	down/down/up	3	1	1	2	3	4	3
	down/up/down	0	0	0	0	0	0	0
	up/down/down	0	0	0	0	0	0	0
	similar	62	82	81	78	65	60	59
	opposite	9	8	7	6	7	9	7
	ratio (similar/opposite)	6.89	10.25	11.57	13.00	9.29	6.67	8.43

Supplemental Table 2 - continued

Comparison		No. of genes similar in CC4348 (*sta6*) at each time point in N-free media (h)						
		0.5	**2**	**4**	**8**	**12**	**24**	**48**
-S/-N	**up/up**	84	152	162	161	162	161	167
	down/down	108	275	225	219	229	179	219
	ratio (up/down)	0.78	0.55	0.72	0.74	0.71	0.9	0.76
	up/down	32	27	20	23	24	25	20
	down/up	29	49	57	66	48	46	45
	similar	192	427	387	380	391	340	386
	opposite	61	76	77	89	72	71	65
	ratio (similar/opposite)	3.15	5.62	5.03	4.27	5.43	4.79	5.94
-P/-N	**up/up**	39	79	83	82	84	90	92
	down/down	16	43	41	39	40	34	38
	ratio (up/down)	2.44	1.84	2.02	2.1	2.1	2.65	2.42
	up/down	18	13	9	8	7	5	6
	down/up	1	1	1	1	1	2	2
	similar	55	122	124	121	124	124	130
	opposite	19	14	10	9	8	7	8
	ratio (similar/opposite)	2.89	8.71	12.40	13.44	15.50	17.71	16.25
-S/-P/-N	**up/up/up**	21	44	43	43	43	46	46
	down/down/down	13	37	36	34	35	30	34
	ratio (up/down)	1.62	1.19	1.19	1.26	1.23	1.53	1.35
	up/up/down	6	1	1	1	1	0	0
	up/down/up	0	0	0	0	0	0	0
	down/up/up	2	4	4	3	3	4	4
	down/down/up	1	1	1	1	1	2	2
	down/up/down	0	0	0	0	0	0	0
	up/down/down	0	0	0	0	0	0	0
	similar	34	81	79	77	78	76	80
	opposite	9	6	6	5	5	6	6
	ratio (similar/opposite)	3.78	13.50	13.17	15.40	15.60	12.67	13.33